Multi-hop Performance Analysis of Whisper Cognitive Radio Networks

Quanjun Chen*, Chun Tung Chou*, Salil S. Kanhere*, Wei Zhang†, Sanjay K. Jha*

*School of Computer Science and Engineering,
The University of New South Wales, Sydney, Australia,
Email: {quanc, ctchou, salilk, sanjay}@cse.unsw.edu.au

†School of Electrical Engineering and Telecommunications,
The University of New South Wales, Sydney, Australia,
Email: w.zhang@unsw.edu.au

UNSW-CSE-TR-1013

April 2010

Abstract

Spectrum scarcity has been one of the main challenges that wireless communications face. Cognitive Radio Networks (CRNs) allow secondary users to opportunistically utilize the licensed spectrum that are dedicated to primary users. In 2003, Federal Communications Commission (FCC) has released a spectrum policy called “Interference Temperature model”. Under this model, the secondary users are allowed to access the licensed spectrum simultaneously with the primary users provided that the interference at the primary receiver meets a certain threshold. We refer the Cognitive Radio Networks that employs this model as “Whisper CRNs” (since secondary users have to use lower transmission power to satisfy the interference constraint). In this work, we analyze the performance of multi-hop whisper CRNs and aim to answer the fundamental question: What is the achieved throughput using whisper CRNs and what are the factors that affect the throughput? We consider a set of realistic network protocols including two-ray radio model and fading radio model at the physical layer, and a geographic routing protocol at network layer. The results quantitatively show that, while the primary users are busy, the secondary users using whisper CRNs can achieve a considerably high end-to-end throughput in some cases (compared to the zero throughput in conventional CRNs where secondary users are prohibited from using the channel when primary users are busy). We also show that the radio propagation characteristics and node density of secondary users have a significant impact on the performance of whisper CRNs.

Index Terms

Cognitive Radio Networks; Interference Temperature Model; Whisper CRNs; Performance Analysis.

I. Introduction

With the rapid growth of wireless applications, one of the main challenges that wireless communications face is the wireless spectrum scarcity. The unlicensed spectrum band, e.g., the ISM band, has become crowded with the growing popularity of WiFi and Bluetooth. On the other hand, the licensed spectrum bands have been shown to be under-utilized [1]. Cognitive radio networks (CRNs) have been proposed to solve the spectrum inefficiency problem [2]. CRNs allow secondary users to opportunistically utilize the spectrum band licensed to primary users under the assumption that the secondary users will not interfere with the primary users. In a conventional cognitive radio network, the secondary users only use the spectrum bands that are currently not occupied by the primary users in order to ensure zero interference to the primary users.

However, due to the spatial reuse feature of radio communication, the licensed band can possibly be concurrently reused by the secondary users even when the primary users are busy. In fact, the Federal Communications Commission (FCC) has proposed a scheme called Interference Temperature (IT) model. In this model, the secondary users are allowed to simultaneously utilize the licensed channel with the primary users, but under the condition that the signal interference at the primary receiver is below a threshold [3]. This model clearly enhances the channel access opportunities and therefore improves the throughput of secondary users. However, what is still unclear is how much throughput improvement can be achieved by the IT model and what are the factors that affect the achieved throughput? This paper aims to answer these fundamental questions.

In interference temperature model, the secondary users must reduce their transmission power so as to meet the interference constraints at the primary users. Due to the reduced transmission power, a secondary source may not reach the destination directly in one-hop (especially in a large network), which will often lead to multi-hop communications. We call such networks with possibly reduced transmission power as “Whisper CRNs”. In literature, several works [4], [5], [6] studied the performance of CRNs under interference temperature model. However, all these works have assumed that the secondary source can communicate with the secondary destination directly in one-hop even with the reduced transmission power. Note that, this assumption only applies to reasonably small networks. Several works proposed using secondary users to relay packets for primary users or other secondary users to improve the overall network throughput [7], [8], [9], [10]. These work only assumed a two-hop scenario with one relay node between a source and a destination. Our previous work [11] studied the multi-hop Whisper CRNs and analyzed the performance, but under the assumption of an ideal radio model where no channel fading is

present. Xie et al. [12] considered the fading channel and analyze the performance of multi-hop Whisper CRNs. However, they only present the results for one-dimensional CRNs.

In this paper, we systematically investigate the performance of whisper CRNs in a large scale two-dimensional ad-hoc scenario. Since, the performance of wireless networks depends on the radio propagation characteristics at physical layer, we consider two different popular radio models and aim to study how the radio characteristics affect the performance of whisper CRNs. The first radio model we consider is two-ray ground reflection propagation model, where the signal attenuation between two nodes solely depends on the distance between the two nodes. As a result, the radio coverage of each node is a perfect circle. However, this is not true in most real-world scenarios [13], [14]. Therefore, we also consider a more realistic radio model, i.e. fading model, that captures the random multi-path (or reflections) effect between the pair. The signal attenuation between two nodes becomes a random variable in fading radio model.

At the routing layer, we consider greedy geographic routing. Greedy geographic routing is a well known localized routing scheme used by many routing protocols [15], [16], [17]. The underlying principle of greedy routing is to select the next hop from amongst a node's neighbors, which is geographically closest to the destination. Since, the forwarding decision at a node is only based on the node's local topology (i.e., location information of one-hop neighbors of this node), greedy routing is highly scalable and particularly robust to frequent changes in the network topology.

The main contributions of this work are four-fold:

- We quantitatively show that secondary users can gain great benefits from whisper CRNs. The achieved throughput largely depends on the locations of secondary pairs and the primary users. Particularly, the secondary users can achieve high throughput when the secondary source is close to the secondary destination, or the secondary communicating pair is far away from the primary communicating pair.
- The analysis results illustrate that the radio models have a great impact on the performance. The secondary users in ideal radio model can achieve better throughput (compared to fading radio) in the scenarios where the source is close to the destination or when the secondary pair is far away from the primary pair. However, the performance in fading radio model outperforms that in the ideal radio model when node density is higher (since random fading can make packets progress a larger distance in one hop in denser networks and therefore less number of hops is required to reach the destination).
- We show that, in fading channel, the performance of whisper CRNs largely depends on the reliability

requirement of primary users. When the reliability requirement is very high, the secondary users have to use a very small transmission power in order to reduce its interference at primary receiver. This leads to a marginal throughput gain for secondary users.

- The analytical results show that the node density affects the performance of whisper CRNs significantly. When the density is low, we can improve the throughput dramatically by deploying more secondary nodes. However, after a certain density value, further increase of node density can only benefit the end-to-end throughput marginally.

The performance analysis of whisper CRNs has its practical implications and can be capitalized in designing efficient CRNs. For example, in our previous work [11], we have shown how to apply the analysis results (based on ideal radio model) to design a multi-channel selection scheme that can achieve minimum channel switch overhead. In a similar vein, we also apply the analysis results of this paper to the multi-channel selection scheme and shown the impact of fading channel on the selection scheme.

The rest of paper is organized as the following. We introduce the system model in Section II. Since the hop count from a secondary source to a destination is a key element in our performance evaluation, we analyze the hop count of a secondary communication pair in Section III. We then study the performance of whisper CRNs in Section IV. In Section V, we apply the analysis result to propose an channel assignment scheme. Finally, Section VI concludes the paper.

II. System Model

The CRNs considered in this paper consist of two types of users: primary and secondary. Primary users have the right to access the licensed spectrum while secondary users are required to ensure that the reception of primary users is not affected. In order to analytically study the performance of CRNs, we assume a 2-dimensional network. The methodology described in this paper can readily be extended to 3-dimension except that the computational requirement will be higher. Fig. 1 depicts a typical example of our CRN. We assume that the primary transmitter (node m) and primary receiver (node n) are fixed at certain locations. The secondary nodes are assumed to be randomly distributed according to a homogeneous Poisson point process with a density of ρ nodes per unit area. Note that, notations will be defined when they are introduced.

At the physical layer of each node (including both primary users and secondary users), we consider two different radio models that have been widely used in the literature: 1) ideal radio model and 2) fading radio model. In the ideal radio model, if the transmission power of node u is P_u, then the received radio

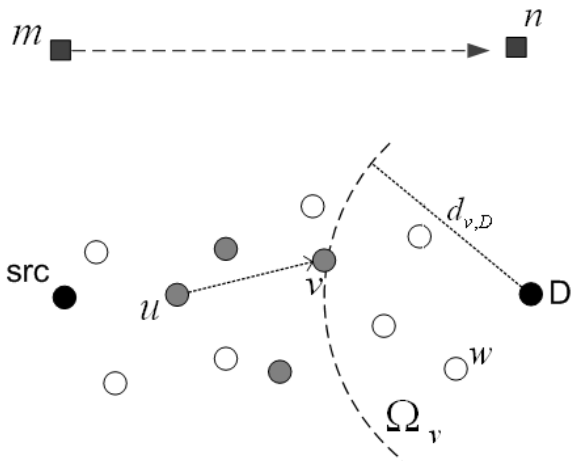

Fig. 1. Typical example of CRN considered in this paper. We use squares to represent primary users and circles to represent secondary users.

power at node v, denoted as $P_v^{'}$, is given by

$$P_v^{'} = \frac{P_u}{d_{u,v}^{\alpha}} \tag{1}$$

where $d_{u,v}$ is the distance between the two nodes u and v, and α is the path-loss exponent. Typical value of α is in the range of $[2, 6]$. Since the received power is a deterministic function of the distance separating the transmitter and the receiver, any two nodes that experience the same distance would have the same attenuation. However, this isotropic propagation has been shown to be unrealistic in most real-world environments. Therefore, we also consider a more realistic radio model, i.e. fading radio model, that accounts for random signals caused by multi-path propagation. We assume the use of Rayleigh flat-fading model in this paper. In such a model, the received power at node v is exponentially distributed and the probability density function follows

$$f(P_v^{'}) = \frac{1}{E(P_v^{'})} \exp\left(-\frac{1}{E(P_v^{'})}\right) \tag{2}$$

where $E(P_v^{'})$ is the mean value and follows $E(P_v^{'}) = \frac{P_u}{d_{u,v}^{\alpha}}$. Note that, for the same pair of nodes, the mean received power is the same as that in the ideal radio model but the actual received power at the receiver fluctuates around this mean value.

We assume that there is a direct link between secondary nodes u and v when the Signal to Noise and Interference ratio (SNIR) at receiver v is no less than a threshold β_S. Let link probability $P_{\wedge}(u, v)$ be

the probability that there is a direct link between u and v (i.e. v is a neighbor of node u). We have,

$$P_{\wedge}(u,v) = Prob\{SNIR_{u,v} \geq \beta_S\} \tag{3}$$

In whisper CRN, the secondary transmitter can access the channel simultaneously with the primary transmitter m. Therefore, the secondary receiver v suffers from the interference caused by the primary transmitter m. Assume that the transmission power of m is P_m. In ideal radio model, the interference from node m is $\frac{P_m}{d^{\alpha}_{m,v}}$. The SNIR at node v is

$$SNIR_{u,v} = \frac{\frac{P_u}{d^{\alpha}_{u,v}}}{N_0 + \frac{P_m}{d^{\alpha}_{m,v}}} \tag{4}$$

where N_0 is the noise level. Since, $SNIR_{u,v}$ here is a deterministic function, the probability that $SNIR_{u,v} \geq \beta_S$ is either one or zero. The link probability follows

$$P_{\wedge}(u,v) = \begin{cases} 1 & \text{if } \frac{\frac{P_u}{d^{\alpha}_{u,v}}}{N_0 + \frac{P_m}{d^{\alpha}_{m,v}}} \geq \beta_S, \\ 0 & \text{otherwise.} \end{cases} \tag{5}$$

In fading radio model, since the received power is a random variable, $SNIR_{u,v}$ is also a random variable. The link probability, given by [18], follows,

$$P_{\wedge}(u,v) = Prob\{SNIR_{u,v} \geq \beta_S\} = \exp\left(-\frac{\beta_S N_0 d^{\alpha}_{u,v}}{P_u}\right) \times \frac{1}{1 + \beta_S \frac{P_m}{P_u}(\frac{d_{u,v}}{d_{m,v}})^{\alpha}} \tag{6}$$

In whisper CRN, the secondary users can transmit packets simultaneously with the primary users. However, the transmission power of the secondary users is constrained so that it will not compromise the reliable transmission of primary users. Now we proceed to estimate the transmission power of secondary user u

In ideal model, we assume that the transmission of primary users is reliable if SNIR at the primary receiver is no less than the threshold β_P. Note that, the primary receiver n suffers from the interference caused by the secondary user u, which is $\frac{P_u}{d^{\alpha}_{u,n}}$. Therefore, the transmission power of secondary user P_u should satisfy

$$SNIR_{m,n} = \frac{\frac{P_m}{d^{\alpha}_{m,n}}}{N_0 + \frac{P_u}{d^{\alpha}_{u,n}}} \geq \beta_P \tag{7}$$

Re-arranging the equation, we have,

$$P_u \leq d^{\alpha}_{u,n}\left(\frac{P_m}{\beta_P d^{\alpha}_{m,n}} - N_0\right) \tag{8}$$

In the case of fading radio model, the transmission of primary users is reliable if the probability that $SNIR_{m,n} \geq \beta_P$ is no less than a reliability threshold γ. We have,

$$Prob\{SNIR_{m,n} \geq \beta_P\} \geq \gamma \tag{9}$$

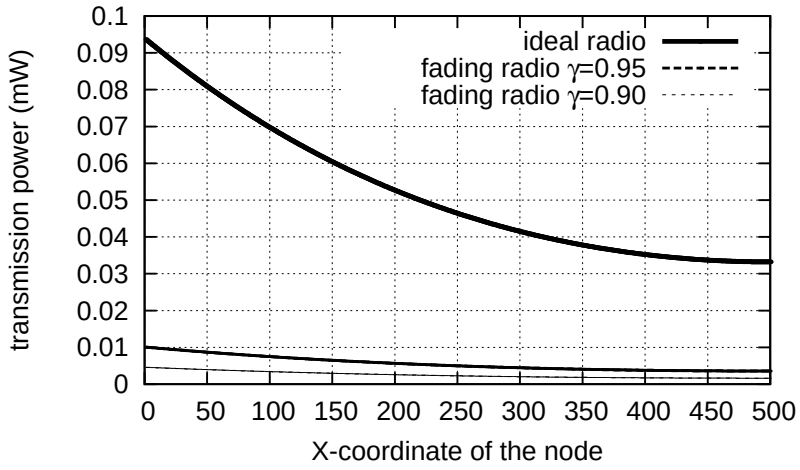

Fig. 2. Maximum allowed transmission power of a secondary user in whisper CRNs as a function of X-coordinate of this user (Y-coordinate is fixed at zero). The coordinates are measured in meters. $P_m = 27dBm$, $N_0 = -90dBm$, $\alpha = 3$, $\beta_P = \beta_S = 15$

The term $Prob\{SNIR_{m,n} \geq \beta_P\}$ can be calculated by the following equation, which is similar to Eq. (6) but here the interference source is secondary user u,

$$Prob\{SNIR_{m,n} > \beta_P\} = \exp\left(-\frac{\beta_P N_0 d_{m,n}^{\alpha}}{P_m}\right) \times \frac{1}{1+\beta_P \frac{P_u}{P_m}(\frac{d_{m,n}}{d_{u,n}})^{\alpha}} \tag{10}$$

Combining Eqs. (9) and (10), the transmission power of secondary node u should satisfy,

$$P_u \leq \frac{P_m}{\beta_P}(\frac{d_{u,n}}{d_{m,n}})^{\alpha}\left\{\frac{1}{\gamma}\exp\left(-\frac{\beta_P N_0 d_{m,n}^{\alpha}}{P_m}\right) - 1\right\} \tag{11}$$

The above discussion shows that the transmission power of a secondary user depends on the locations of the secondary user, primary transmitter and primary receiver. Now we illustrate the transmission power of a secondary user using numerical results calculated by Eqs. (8) and (11). We assume $P_m = 0.5W(27dBm)$, $N_0 = 1.0E-12W(-90dBm)$, $\alpha = 3$, $\beta_P = \beta_S = 15$, and the primary transmitter and receiver are located at (0,500) and (500,500) respectively. The coordinates are measured in meters. We will use this set of parameters throughput the paper. For the fading radio, we consider two cases: $\gamma = 0.90$ and $\gamma = 0.95$. We vary the x-coordinate of secondary users from 0 to 500 and fix the y-coordinate at 0. Fig. 2 compares the maximum allowed transmission power of the secondary users for different radio models. It shows that, for both ideal and fading models, the transmission power decreases with the x-coordinate of secondary node. When the x-coordinate of secondary user increases from 0 to 500, the node is closer to the primary receiver and will hence introduce more interference at the primary receiver. Therefore, the node needs to use a smaller transmission power in order to keep the interference at the primary receiver under the

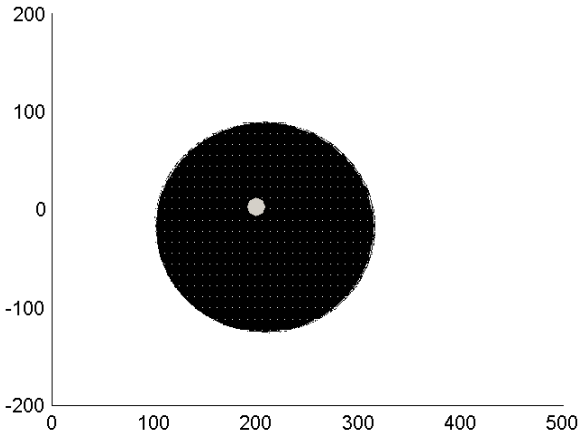

Fig. 3. Link probability from a node at location (200,0) to a node at any other location under ideal radio model. Dark area is the radio coverage of the node, within which the link probability at each location is one.

constraint. Comparing the different radio models, Fig. 2 shows that the node in fading radio requires significantly less transmission power than in ideal radio. This is due to the fact that, in fading radio, the received power at primary receiver is a random variable. As a result, the instantaneous SNIR at primary receiver has a wide range of values. In order to keep the instantaneous SNIR above the required value in most cases (with the value of γ), we need to ensure a very small interference from the secondary user and therefore a much smaller transmission power. Clearly, the transmission power in fading channel also depends on the reliability threshold γ. With a high value of γ, we have a tighter interference constraint and therefore further reduce the transmission power of the secondary user, as shown in Fig. 2.

Knowing the transmission power of secondary users, we can substitute it into Eqs. (5) and (6) to compute the link probability for any two secondary users. Here we assume that secondary users employ the maximum allowed transmission power given by Eqs. (8) and (11). Fig. 3 illustrates the link probability from a node u at location (200,0) to a node at any other location under ideal radio model. The node u in the figure is represented as a small grey circle located at (200,0). Recall that, the link probability in ideal radio model is either one or zero. The dark region in Fig. 3 represents the radio coverage of node u, inside which the link probability is one. In other words, all the nodes inside the coverage are the neighbors of u. The figure illustrates that, the radio coverage is close to a disk shape but node u is

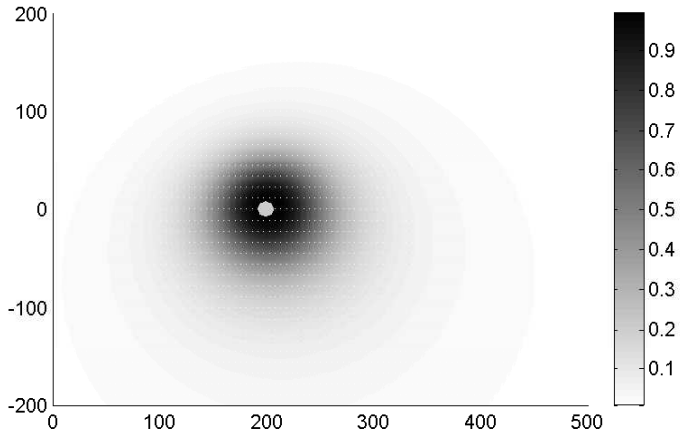

Fig. 4. Link probability from a node at location (200,0) to other location under fading radio model. The color at each location denotes the value of link probability from (200,0) to this location.

not the center of the disk. This is the result of interference from primary transmitter [1]. Similarly, Fig. 4 illustrates the link probability from node u to other locations under fading radio model. The grey level at each location represents the value of link probability, which varies between 0 and 1. In contrast to ideal radio, we do not have a clear radio coverage in fading radio. The neighbors of node u can be located at any place in the network. Of course, when a node is closer to node u, the node has larger chance to become a neighbor of u. Both Fig. 3 and Fig. 4 illustrate that a secondary user may not have a direct link to the destination, which leads to multi-hop communication. Next, we analyze the the number of hops required from a secondary source to a secondary destination in whisper CRNs.

III. Analysis of Hop Count

This section seeks to develop a model for analyzing the hop count from the secondary source to the secondary destination in a whisper CRN when the primary users are busy.

We use a discrete Markov chain to model the hop-by-hop progress of a packet from the source to the destination. The state of the Markov chain is defined as the location of the current forwarding node that holds the packet. Consider the network in Fig. 1 where the node u located at (x_u, y_u) is currently holding the packet. The neighbors of u are represented by grey circles. In greedy routing, a forwarding node

[1]In the absence of the interference from primary transmitter, the radio coverage should be a perfect circular area with node u as the center of the circle.

selects the next hop from amongst its neighbors that is geographically closest to the destination. Since node v is the closest neighbor to the destination in this example, Node u chooses v located at (x_v, y_v) as the next hop. We model this packet movement from nodes u to v as a state transition from (x_u, y_u) to (x_v, y_v). In general, the hop-by-hop progress, that is made by a packet towards the destination, can be represented by a series of state transitions that eventually culminates in state (x_d, y_d), which are the coordinates of the destination D. The number of hops from a source to a destination is the number of states the packet goes through.

Note that, ideally the states in this Markov chain should be modeled as a continuous random variable. However, to simplify our model, we use a discrete state space to approximately represent the continuous values. We divide the two-dimensional network area into a grid, each cell of which has a length of ε and a width of ε, where the parameter ε is the interval of the state space (i.e. the quantization coefficient). When the interval ε is small enough, the discrete state space approximates the original continuous space. In the rest of paper, when we refer "a node (or no node) at location (x, y)", we actually mean "a node (or no node) within the small cell around (x, y)".

Our analysis is composed of the following steps. The first step involves determining the state transition probabilities for the Markov chain (section III-A) using geometric calculation. Based on the transition probabilities, we recursively compute the hop count distribution and the mean value given a communication pair (Section III-B). Finally, we propose an approximation to simplify the analysis and reduce the computational complexity (Section III-C). Note that, the analysis is independent of the radio model under consideration. One simply has to substitute the appropriate link probability equations as derived in the previous section for the radio model under consideration.

A. State Transition Probability

The aim of this section is to derive an expression for the state transition probability, which will be used in the next section to derive a probability density function of the hop count for greedy geographic routing in whisper CRN.

As illustrated in Fig. 1, the state transition from (x_u, y_u) to (x_v, y_v) is the joint event that node u has at least one neighbor located at (x_v, y_v) and no neighbors located closer to the destination than (x_v, y_v). Since, if there exists a neighbor located closer than (x_v, y_v) to the destination, any node in (x_v, y_v) will not be chosen by geographical routing. Let Ω_v denote the region containing all the points that are closer to destination than node v, as illustrated in in Fig. 1. Therefore, the probability that current node u will send the packet to a node v is the probability of the joint event that there are no neighbors within Ω_v

and there is at least one neighbor at (x_v, y_v). Note that, there should also be no direct link from node u to the destination. Otherwise, the packet will be forwarded to the destination directly skipping state (x_v, y_v). We have the following theorem.

Theorem 1: We assume that the destination D is located at (x_d, y_d) and the current state of a packet is at (x_u, y_u), which corresponds to a secondary node u situated at this location. Let $d_{u,D}$ and $d_{v,D}$ be the distance from location (x_u, y_u) and (x_v, y_v) to D respectively. In whisper CRN, the transition probability of a packet from current state (x_u, y_u) to next state (x_v, y_v) is,

$$P_{(x_u,y_u)->(x_v,y_v)} = \begin{cases} 0 & \text{if } d_{u,D} \leq d_{v,D}, \\ \eta & \text{otherwise} \end{cases} \tag{12}$$

where

$$\eta = \Big[1 - P_{\wedge}(u, D)\Big]\Big[1 - \exp\left(-\rho\epsilon^2 P_{\wedge}(u, v)\right)\Big] \prod_{(x_w,y_w)\in\Omega_v} \exp\left(-\rho\epsilon^2 P_{\wedge}(u, w)\right) \tag{13}$$

and $P_{\wedge}(u, v)$ is the link probability from a node at (x_u, y_u) to a node at (x_v, y_v), defined in Eq. (5) and (6) for ideal radio model and fading radio model respectively. Ω_v is the set of all locations that are closer to destination D than location (x_v, y_v).

Proof: According to greedy routing, the next state (x_v, y_v) should be always closer to the destination than current state (x_u, y_u), i.e. $d_{u,D} > d_{v,D}$. In other words, the node u would never forward a packet to (x_v, y_v) if (x_v, y_v) is further away from the D than (x_u, y_u). Hence, the transition probability is zero if $d_{u,D} \leq d_{v,D}$, which explains the first case in Eq. (12).

For the second case, as we have discussed, the transition probability is the product of the following three independent probabilities.

$$\begin{aligned} P_{(x_u,y_u)->(x_v,y_v)} = \quad & Prob\{\text{no direct link from node } u \text{ to the destination}\} \\ & \times Prob\{\text{at least one neighbor at } (x_v, y_v)\} \times Prob\{\text{no neighbor within } \Omega_v\} \end{aligned} \tag{14}$$

The first term in the right side of Eq. (14) can be easily calculated as,

$$Prob\{\text{there is no direct link from node } u \text{ to the destination}\} = 1 - P_{\wedge}(u, D) \tag{15}$$

Now we compute the the second term in Eq. (14). The probability of at least one neighbor existing at (x_v, y_v) is the complementary probability that no neighbor is located at (x_v, y_v).

$$Prob\{\text{at least one neighbor at } (x_v, y_v)\} = 1 - Prob\{\text{no neighbor at } (x_v, y_v)\} \tag{16}$$

The event that no neighbor is located at (x_v, y_v) is the event that, for any k number of nodes at (x_v, y_v), there are no direct links from u to any one of these k nodes. Therefore,

$$\begin{aligned} Prob\{\text{no neighbor at } (x_v, y_v)\} &= \sum_{k=0}^{\infty} \Big\{ Prob\{\text{there are k nodes at } (x_v, y_v)\} \times \\ & \qquad Prob\{\text{there is no direct link from } u \text{ to any one of these k nodes}\} \Big\} \end{aligned} \tag{17}$$

Since, we assume a discrete state space with ε as the quantization interval, we can approximate point (x_v, y_v) as a small square with area of ϵ^2. Therefore, when we refer to "k node at location (x, y)", we actually mean "k node within the small cell around (x, y)". Recall that, nodes follow Poisson distribution. The number of nodes within an area of ϵ^2 follows a Poisson distribution with mean of $\rho\epsilon^2$. The probability that there are k nodes in the (x_v, y_v) is

$$Prob\{\text{there are k nodes at } (x_v, y_v)\} = \frac{(\rho\epsilon^2)^k \exp(-\rho\epsilon^2))}{k!} \tag{18}$$

Given there are k nodes at (x_v, y_v), the link probabilities from u to any one of these nodes are independent of each other. Knowing the link probability $P_\wedge(u, v)$, we have,

$$Prob\{\text{there is no direct link from } u \text{ to any one of these k nodes}\} = (1 - P_\wedge(u, v))^k \tag{19}$$

Substituting Eqs. (18) and (19) into (17), we have,

$$\begin{aligned} & Prob\{\text{no neighbor at } (x_v, y_v)\} = \sum_{k=0}^{\infty} \frac{(\rho\epsilon^2)^k \exp(-\rho\epsilon^2))}{k!} \times (1 - P_\wedge(u, v))^k \\ & = \exp(-\rho\epsilon^2 P_\wedge(u, v)) \sum_{k=0}^{\infty} \frac{[\rho\epsilon^2(1 - P_\wedge(u, v))]^k \exp[-\rho\epsilon^2(1 - P_\wedge(u, v))]}{k!} \\ & = \exp(-\rho\epsilon^2 P_\wedge(u, v)) \end{aligned} \tag{20}$$

Next, we compute the the third term in the right side of Eq. (14), i.e. the probability that node u does not have any neighbor within region Ω_v. This probability is the probability of joint events that, for any location within Ω_v, e.g. (x_w, y_w), there is no neighbor at this location. We have,

$$Prob\{\text{no neighbor within } \Omega_v\} = \prod_{(x_w, y_w) \in \Omega_v} Prob\{\text{no neighbor at } (x_w, y_w)\} \tag{21}$$

The variable $Prob\{\text{no neighbor at } (x_w, y_w)\}$ can be computed in the same way as Eq. (20). Combining Eqs. (14), (15), (16), (20) and (21), the theorem can be proved.$\triangle$ $\triangle\triangle$

B. Hop Count Distribution and Mean Value

Based on the transition probability computed earlier and using recursive computation, we have the following results on the probability density function of the hop counts.

Theorem 2: Given a secondary node u (located at (x_u, y_u)) and a destination D (at (x_d, y_d)), the probability distribution of hop count H (an integer variable) in greedy routing from u to D is given by,

$$P(H = h|(x_u, y_u), (x_d, y_d)) = \begin{cases} P_{\wedge}(u, D) & \text{if } h = 1, \\ \xi & \text{if } h > 1 \end{cases} \tag{22}$$

where

$$\xi = \sum_{(x_v, y_v)} P_{(x_u, y_u)->(x_v, y_v)} P(H = h - 1|(x_v, y_v), (x_d, y_d)) \tag{23}$$

and $P_{(x_u, y_u)->(x_v, y_v)}$ is the state transition probability given in Theorem 1, $P(H = h-1|(x_v, y_v), (x_d, y_d))$ is the probability that the hop count from a node at (x_v, y_v) to destination D is $h - 1$. $\triangle\ \triangle\triangle$

Proof: Note that, if the hop count from the current state (x_u, y_u) to the destination is h, then hop count from the next state (x_v, y_v) to the destination must be $h - 1$. By applying the law of total probability, we have the recursion in Eq. (23). For the case of $h = 1$, the one-hop probability is the probability that there is a direct link from node u to the destination. $\triangle\ \triangle\triangle$

Since, the state transition probabilities depend on the link probabilities, which are functions of the network parameters, e.g. node density, the locations and transmission power of primary users etc. (given in Eq. (5) and (6)), the hop count distribution is also a function of these parameters. However, for brevity, we will not make these dependencies explicit. The result of Theorem 2 shows that we can use recursive computation to obtain the probability density function of the hop-count for a given secondary source-destination pair.

We can use the hop count density function to derive *path availability* and *mean hop count.*

1) Path availability: Note that, there is a chance that a source may not be able to find a routing path to a destination. This is due to the failure of greedy forwarding, where no neighbor is closer to the destination than the forwarding node itself[2]. For a given pair of source and destination, if we sum the hop count probabilities over all hop count values, the result is the probability that the source can successfully find a routing path to the destination. We denote the summation as V, and refer it as the

[2]In conventional geographic routing protocol, other forwarding schemes, e.g. face routing [15], are used when the greedy routing fails. We do not consider these recovery schemes for simplicity.

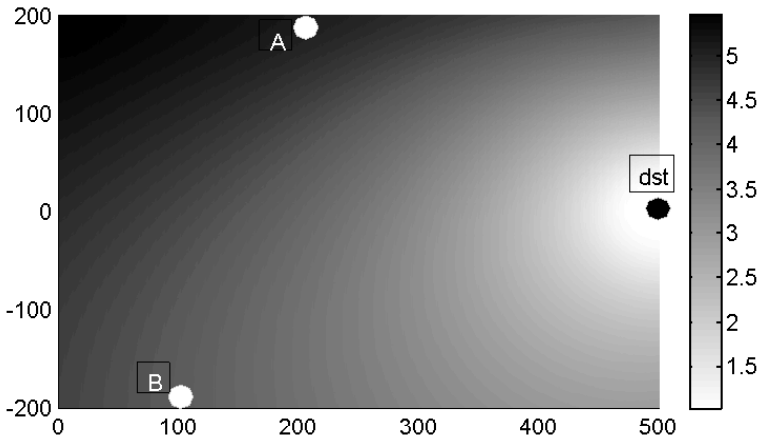

Fig. 5. Mean hop count as a function of source location under fading radio model. The destination is located at (500,0). Primary transmitter and primary receiver are located at (0,500) and (500,500) respectively. The coordinates are measured in meters. $P_m = 27dBm$, $N_0 = -90dBm$, $\alpha = 3$, $\beta_P = \beta_S = 15$, $\gamma = 0.9$

path availability from the source S to the destination D. We have,

$$V = \sum_{h=1}^{\infty} P(H = h|(x_s, y_s), (x_d, y_d)) \tag{24}$$

2) Mean hop count: Now we proceed to compute the mean hop count for a given communicating pair. Note that, the hop count is only meaningful when there is a routing path from the source to the destination. Therefore, when we calculate the mean hop count, we only consider the case that the source can successfully find a routing path to the destination.

Based on Theorem 2, the probability that the hop count is h is $P(H = h|(x_s, y_s), (x_d, y_d))$. Consequently, the probability that the hop count is h on the condition that there is a routing path, is $P(H = h|(x_s, y_s), (x_d, y_d))/V$. Finally, the mean hop count $\overline{H}$ on the condition that there is a routing path is:

$$\overline{H} = \frac{\sum_{h=1}^{\infty} h \cdot P(H = h|(x_s, y_s), (x_d, y_d))}{V} \tag{25}$$

We illustrate the mean hop count given by Eq. (25) using a numerical example. We assume that the secondary destination is located at (500, 0). The primary transmitter and receiver are located at (0,500) and (500,500) respectively. The unit of the $x - y$ coordinates is meters. Node density is $\rho = 0.0005$ per square meters. The quantization interval is $\varepsilon = 1m$. Other parameters are the same as those used in Fig. 2. Fig. 5 shows the mean hop count from the different source locations to the destination under fading channel, where the reliability threshold γ is 0.9. The level of grey at a location indicates the

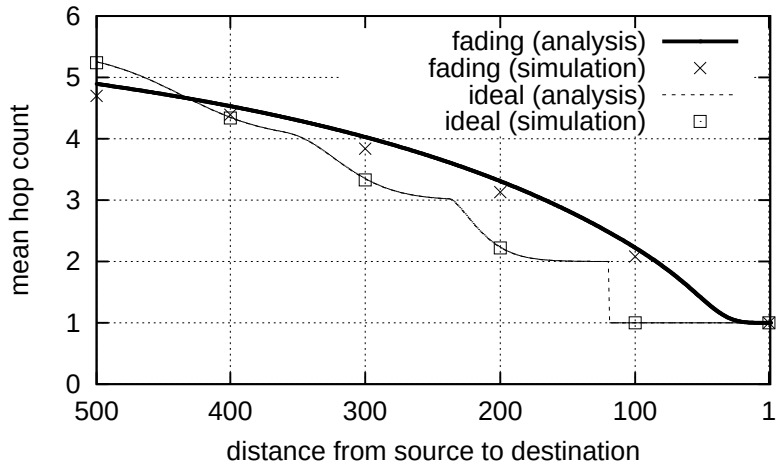

Fig. 6. Mean hop count as a function of source-to-destination distance.

mean hop count from this location to the destination. This figure clearly shows the impact of primary pair on the hop count. Note that, in a traditional wireless ad hoc network (no primary users), when the source is further away from the destination, it generally takes longer hops to reach to the destination [19]. However, Fig. 5 shows that this rule does not hold when there exists power constraints and interference due to primary users. For example, although location A in the figure (360m from the destination) is closer to the destination than the location B (450m from the destination), a node at location A takes more hops on average (5.1 hops) to reach the destination than the source at location B (4.2 hops). This is due to the non-uniform transmission power of the secondary users. In this example, location A is closer to the primary receiver. Hence, it is forced to use a smaller transmission power in order to satisfy the interference constants at the primary receiver. A smaller transmission power leads to a smaller radio coverage and therefore more hops to reach the destination.

In order to validate the correctness of the analytical model, we develop a custom C++ simulator to simulate the hop count results. In the simulation, the nodes are randomly distributed according to a homogeneous Poisson point process. The network parameters are the same as we use in producing the analysis results in Fig. 5. The destination is fixed at (500,0) but we vary the location of the source from (0,0) to (500,0) (along x axis). For each secondary node, the transmission power is determined by Eq. (8) or (11) for the different radio models. The simulator constructs the neighbor list for each secondary node, i.e. for a node u, if the SNIR at another node v is no less than the threshold β_S, the node v is included in the neighbor list of u. Based on the neighbor list of each node (local topology), we

then use greedy routing to find the routing path from a source to a destination and count the number of hops. The comparisons between the analysis results and the simulation results are depicted in Fig. 6. The figure shows that the simulation results are in line with the analysis results, which justifies our analytical model. Note that, in ideal radio model, the mean hop count drops sharply from 2 to 1 when the source is about 120m away from the destination. The reason is that, when the source-to-destination distance is more than 120m, the source cannot reach the destination directly and needs at least one relay node. Therefore, the hop count is at least 2. However, when the distance is less than 120m, the source can directly communicate with the destination and therefore the hop count drops to 1. In fading radio model, we do not observe this sharp decrease. This because, even if the source-to-destination distance is less than 120m, the source may not always have a direct link to the destination due to the random fading and therefore the average hop count is greater than one.

Fig. 6 also shows another interesting pattern when comparing the hop count results of two different radio models. When the source is close to the destination, the node in fading radio model takes more hops than it does in ideal radio model. On the contrary, when the source is further away from the destination, the fading radio model incurs a smaller number of hops. We will explain the reasons for this result in the next subsection (see Section III-C).

Note that, the above computation of the mean hop count requires us to recursively compute the hop count distribution at each location in the entire 2-dimensional space. This computation has a time complexity of $O(d^3)$, where d is the distance between the source and destination. It is evident that evaluating the mean hop count for a sizable network can be a considerably computationally intensive task. Hence, in the next section, we derive a simplified technique to estimate the mean hop count.

C. Approximation of Mean Hop Count

In order to compute the mean hop count approximately, we introduce the concept of *hop distance*, which measures the progress made by a packet towards the destination in one hop. If we can estimate the average hop distance along the routing path, denoted as $\overline{\delta}$, we can approximate the mean hop count as the ratio of the source-to-destination distance to the average hop distance.

$$\overline{H} = \frac{d_{(x_s,y_s),(x_d,y_d)}}{\overline{\delta}} \tag{26}$$

In order to calculate the average hop distance along the routing path, we need to know the hop distance when the packet is at any intermediate location (x, y). This can be derived from the state transition probability presented in Theorem 1. Let $d_{u,D}$ be the distance from the current location (x_u, y_u) to the

destination, and $d_{v,D}$ be the distance from the next state (x_v, y_v) to the destination. The hop distance can be calculated as follows,

$$\delta(x_u, y_u) = \sum_{(x_v,y_v)\in\Omega_u} (d_{u,D} - d_{v,D}) P_{(x_u,y_u)->(x_v,y_v)} \tag{27}$$

It is worth noting that the mean hop count is the average hop count on the condition that there is a routing path from the source to the destination. Similarly, when we calculate hop distance, we should also consider the condition that each intermediate forwarding node can successfully find a next hop. Let $W(x_u, y_u)$ be the probability that a node at location (x_u, y_u) can successfully find the next hop, referred as *link success probability*. According to greedy routing, $W(x_u, y_u)$ is the complimentary probability that the node does not have neighbor closer to the destination than the node itself. Let ω_u denote the region that includes all the locations that are closer to the destination than the node u itself. We have,

$$W(x_u, y_u) = 1 - Prob\{\text{no neighbor within } \Omega_u\} \tag{28}$$

The unknown parameter $Prob\{\text{no neighbor within } \Omega_u\}$ can be calculated in the same way as shown in Eq. (21). Therefore, we have,

$$W(x_u, y_u) = 1 - \prod_{(x_w,y_w)\in\Omega_u} Prob\{\text{no neighbor at } (x_w, y_w)\} \tag{29}$$

Therefore, the hop distance at (x_u, y_u) given that the next hop exists is:

$$\delta(x_u, y_u) = \frac{\sum_{(x_v,y_v)\in\Omega_u} (d_{u,D} - d_{v,D}) P_{(x_u,y_u)->(x_v,y_v)}}{W(x_u, y_u)} \tag{30}$$

Fig. 7 illustrates the hop distance of the intermediate node u for both radio models. We vary the location of node u from (0,0) to (500,0). The figure shows that when node u is closer to the destination, the hop distance in fading radio is smaller than that in ideal radio. On the contrary, when the location is further from the destination (more than 230m away), the fading radio generates larger hop distance. This behavior is caused by the random characteristics of fading channel. Because of the random signal, two nodes that are closer to each other do not necessarily have a direct link. Therefore, a node that is closer to the destination tends to have smaller hop distance in fading radio (therefore a larger hop count in the right side of Fig. 6). Similarly, due to the random signal in fading radio, two nodes that are further away from each other can still possibly have direct link between them. Therefore, when a node is far from the destination, the node can potentially find neighbors that are distant from the node itself and therefore achieve larger hop distance. The larger hop distance in fading radio leads to smaller number of hops, which explains the shape of the curves in the left side of Fig. 6. Note that, in Fig. 7, the hop distance

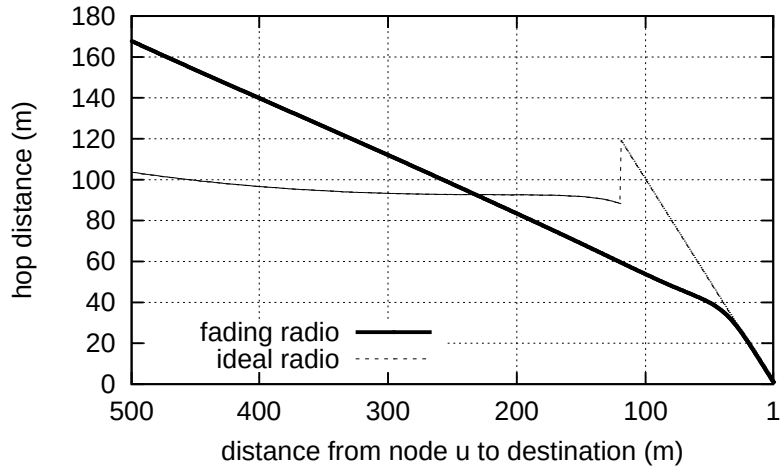

Fig. 7. Hop distance of an intermediate node u (represented as the distance from u to the destination)

for ideal radio model increases dramatically at about 120m. This is due to the fact that, when the node is further away from destination than 120m, the node cannot reach the destination directly and the hop distance is around 90m (according to (30)). However, when the node is at 120m, the node can directly communicate with the destination and therefore the hop distance increases to 120m.

Now we calculate the average hop distance $\overline{\delta}$ from a source to a destination. We assume that all the intermediate forwarding nodes are located along the straight line connecting the source and destination [3]. Therefore, the average hop distance is the average value of hop distance over all the locations along the routing path. Let Ω be the set of locations that lie on the straight line connecting the source and destination. We have,

$$\overline{\delta} = \frac{\sum_{(x,y)\in\Omega} \delta(x,y)}{\sum_{(x,y)\in\Omega} 1} \tag{31}$$

As an illustration, we compare the approximation of mean hop count with the exact calculation via Theorem 2. We assume the same network parameters as those used in Fig. 6. Fig. 8 shows the mean hop count when the source varies from location (0,0) to (0,500) (along the x axis). Note that, the destination is fixed at (0,500) and therefore the distance from the source to the destination varies from 500 to 0. In the figure, the thick lines represent the approximation results and the corresponding thin lines represent the exact calculation results. The figure shows that the simplified calculation can approximate the mean hop count with an error of less than 10% on average. However, the computation complexity is reduced

[3]The forwarding nodes in greedy routing are indeed located close to the straight line connecting the source and the destination.

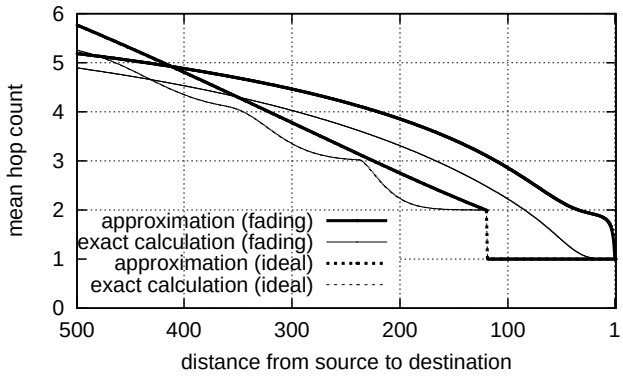

Fig. 8. Approximation of mean hop count as a function of source-to-destination distance

significantly from $O(d^3)$ to $O(d)$ since the recursive computation is now carried out along a line, rather than on a plane.

IV. Performance Results

In this section, we analyze the end-to-end throughput of a secondary communication pair in whisper mode, i.e. when the primary users are busy. We first define the end-to-end throughput. We then investigate the impact of network parameters on the throughput of secondary network, including radio model, the secondary source-to-destination distance, the distance from secondary pair to primary pair and the nodes density.

A. Definition of End-to-End Throughput

We assume that, when a secondary user transmits a packet, all the other secondary nodes keep silent (i.e. no spatial reuse is applied among secondary users)[4]. We further assume that there is only one communicating pair in the network. Under these simplified assumption, the throughput of the pair is the data rate at link layer r divided by the hop count from the source to the destination, i.e. $\frac{r}{H}$. (Note that, we assume that the secondary nodes use a constant transmission rate r at the link layer. One can think of this as the transmission rate that can be supported by SNIR threshold β of the secondary users.) Note

[4]Note that, if we consider the channel reuse, multiple secondary users can utilize the channel at the same time. Therefore, we need a power allocation algorithm to assign power for each of the multiple transmitters so that their collective interference at the primary receive is below the required constraint. We also need a multi-access protocol for collision avoidance between 1-2 hop neighbors. We plan to address this issue in our future work.

that, when the source cannot find a routing path to the destination, the throughput is zero. Therefore, the average end-to-end throughput, E, is

$$E_{whisper} = \frac{r}{\overline{H}} \cdot V \tag{32}$$

where V is the path availability probability measuring the probability that a source can successfully find a routing path to a destination. As discussed in Section III-B, path availability can be calculated by the hop count distribution according to Eq. (24). However, this approach requires a high computation complexity due to the requirement of hop count distribution information. Here, we also propose a simplified approach to estimate the path availability. Recall that, when a packet is making its way to the destination, each intermediate node may fail to find the next hop. Path availability is the joint probability that all the forwarding nodes (including the source) can successfully find a next hop. Recall that, $W(x, y)$ denotes the probability that an intermediate node at location (x, y) can successfully find the next hop. If we know the average value of W per hop, and the mean hop count $\overline{H}$, we can estimate the path availability for the whisper mode by

$$V = \overline{W}^{\overline{H}} \tag{33}$$

Similar to the approximation of mean hop count, we assume that all the intermediate forwarding nodes lie along the straight line connecting the source and destination. Therefore, an approximation for the mean per-hop path availability is

$$\overline{W} = \frac{\sum_{(x,y)\in\Omega} W(x, y)}{\sum_{(x,y)\in\Omega} 1} \tag{34}$$

where Ω has the same meaning as that in Section III-C.

B. Performance Results

In this section, we present the throughput results of secondary users in whisper CRN under two different radio models. We study the impact of network parameters on the end-to-end throughput of secondary pair using numerical results from Eq. (32). We vary the parameters, including the distance from secondary source to secondary destination, the distance from the primary pair to secondary pair, the node density and the reliability requirement of primary users.

We first vary the distance between the secondary source and the secondary destination. We fix the destination at location (500,0) and vary the source from (0,0) to (500,0). Other parameters are the same as those in Fig. 5. We normalize the end-to-end throughput using the link data rate r. Fig. 9 shows the numerical results of the normalized end-to-end throughput as the function of source-to-destination distance. It illustrates that, under the interference constraints, the secondary throughput is relatively low

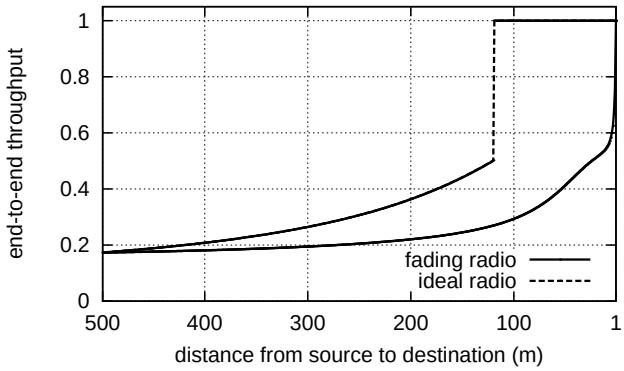

Fig. 9. Impact of secondary source-to-destination distance on the end-to-end throughput

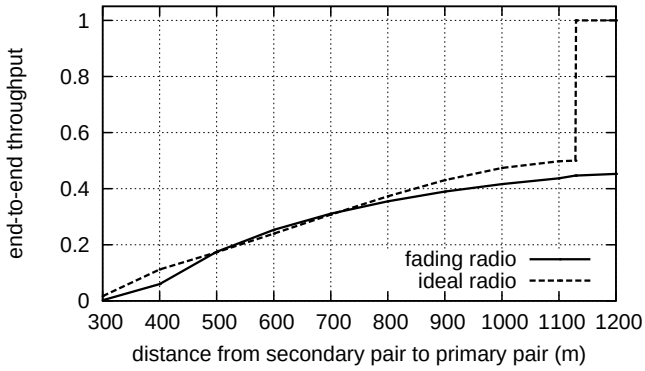

Fig. 10. Impact of distance from the primary pair to the secondary pair on the end-to-end throughput

for a larger source-to-destination distance. It then increases slowly with the distance, until the two nodes are so close that the source may have direct connection with the destination. The sharp increase observed with the ideal radio model is because of the sudden change in the mean hop count from 2 to 1 (see Fig. 6) when the source-destination distance is lower than 120m. As a result, the normalized throughput increases sharply from 0.5 to 1. Note that, when the source is close to the destination, the pair in fading radio has significantly lower throughput than in ideal radio. This is because, due to the random fading, the pair may not have a direct connection even when they are close to each other. As a result, the source may require other relay nodes to forward packets and therefore decreases the end-to-end throughput. In general, the secondary pair can gain greater benefit in the whisper CRNs, when the secondary source is close to the destination.

In the second study, we vary the distance between the primary and secondary pairs. The primary

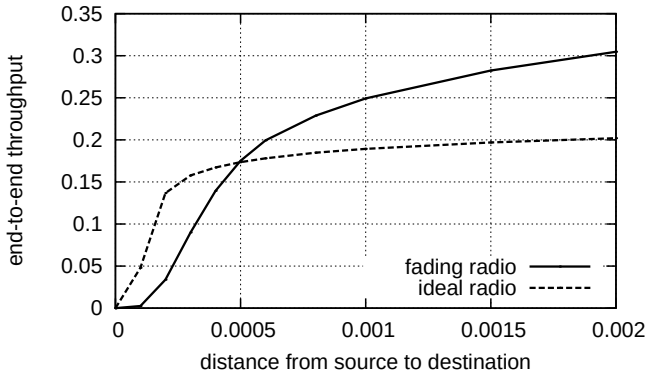

Fig. 11. Impact of node density on the end-to-end throughput

transmitter and receiver are still fixed at (0,500) and (500,500) respectively (the primary pair is parallel to the x-axis). The secondary source and destination are also 500m apart, and are placed in a line parallel to x axis. We vary the y-coordinate of the secondary pair from 200 to -800. Equivalently, the distance from the primary pair to the secondary pair varies from 300m to 1300m. Fig. 10 depicts that, for both radio models, the throughput initially increases linearly with the distance. However, for ideal radio model, after a certain point (distance of 1150m) the secondary pair is so far away from the primary pair that the transmitting power limitation due to the interference constraint disappears. Thus, the secondary source can use the maximum transmission power (0.5W in this example) and communicate directly with the secondary destination. As a result, the end-to-end throughput equals to the link data rate of r. For fading radio model, even with such maximum transmission power, the source still needs the relay nodes to reach the destination and therefore leads to the smaller throughput [5].

Recall that, node density has a great impact on the path availability and therefore on the end-to-end throughput (according to Eq. (32)). Next, we study the actual impact of node density on the throughput. We vary the node density ρ from 0 to 0.002. The source and the destination are located at $(500, 0)$ and $(500, 0)$ respectively. Fig. 11 shows the end-to-end throughput as a function of node density. It shows that, for both radio models, the throughput increases rapidly with an increase in the node density, but the rate of increase slows down considerably before it converges to a maximum value. However, the converged throughput value in fading radio (above $0.35r$) is much higher than the one in ideal radio (about $0.2r$). This is again due to the random signal in fading channel. With high node density, each

[5]Note that, if the source can directly communicate with the destination, the throughput is r. However, if the source needs two hops to reach the destination, the throughput decreases significantly to $0.5r$.

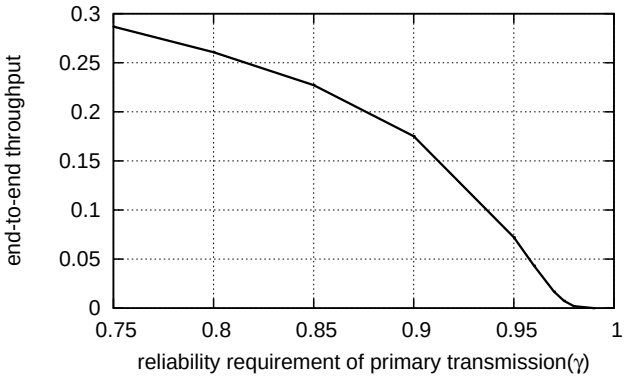

Fig. 12. Impact of reliability requirement (γ) on the end-to-end throughput

node has a better chance of finding neighbor that is distant from the node itself and therefore the node can achieve longer hop distance. This leads to the smaller hop count from the source to the destination and finally larger end-to-end throughput. Generally, the figure shows that, for each radio model, when the density is low, we can improve the throughput dramatically by deploying more secondary nodes. However, after a certain knee point, the further increase of node density can only benefit the end-to-end throughput marginally.

In fading radio, the transmission power of a secondary node is limited so that the interference will not decrease the quality of primary transmission below the reliability requirement, as stated in Eq. (11). Now, we study the effect of the reliability requirement γ on the performance of secondary users. We vary γ from 0.75 to 0.99. The higher value of γ, the stricter interference constraint we have on the secondary users. Fig. 12 shows the normalized throughput as the function of γ. As the expected, the throughput decreases with the reliability requirement. Since, with the higher value of γ, the transmission power of each secondary user has to be smaller in order to satisfy the stricter constraint, as illustrated in the previous Fig. 2. The smaller transmission power leads to longer hops and therefore smaller throughput. When γ increases to 0.98, the throughput is reduced to almost zero. Therefore, in fading radio, whisper CRN can only achieve throughput gain when the primary users have less rigorous reliability requirement.

V. Multi-channel whisper CRNs

Our analysis on the performance of whisper CRNs has assumed only one channel. Intuitively, if we have multiple orthogonal channels scenarios, the secondary users can access these multiple channels simultaneously and therefore improve the network throughput. In this section, we propose and analyze a channel assignment strategy, which works in conjunction with greedy geographic routing.

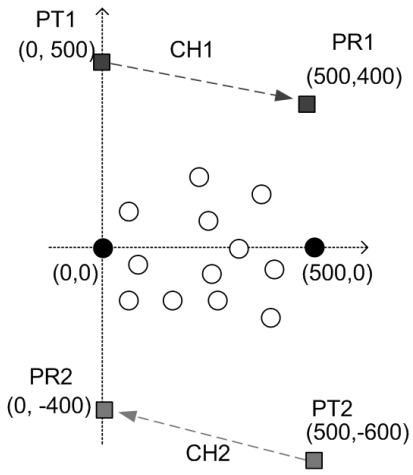

Fig. 13. Example for two primary pairs.

In order to simplify the description, we consider the case with 2 channels. The proposed scheme can be extended to more than two channels. We also assume that both channels have the same link layer data rate. Consider the situation depicted in Fig. 13 where two primary user pairs operate in two channels: channels 1 and 2. Note that, in Fig. 13, the primary receiver of channel 1 is closer to the secondary destination than it is to the secondary source. If a packet is routed to the destination from the source using channel 1 only, as the packet gets closer to the primary receiver, the nodes holding the packets are forced to use a smaller transmission range because they must reduce their transmission power in order not to affect the primary receiver. In order words, the hop distance in channel 1 becomes smaller as it gets closer to the destination. On the other hand, the primary receiver of channel two is closer to the secondary source than it is to the secondary destination. Therefore, if the packet is routed using channel 2 when it is near the destination, then the nodes holding the packet can use a larger transmission range, or longer hop distance. This can improve the end-to-end performance.

We confirm the intuitive argument in the last paragraph by plotting the hop distances of intermediate nodes when using different channels in Fig. 14. The hop distance is calculated by Eq. (27). We use the ideal radio model as an example and assume that node density is 0.001 per square meters. Other parameters are the same as those used in Fig. 2. Similar to the approximate procedure to compute the mean hop count, we assume that the intermediate nodes are located along the straight line from the source to the destination. Fig. 14 shows that there exists a cut off point. To the left side of this point, using channel 1 will give a large hop distance but to the right side of this point, using channel 2 instead

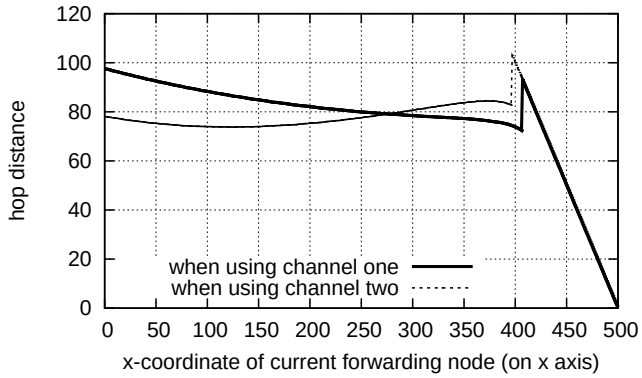

Fig. 14. Hop distance as a function of nodes' location (ideal radio model).

will give a larger hop distance.

This motivates us to propose a channel assignment strategy which can readily work with greedy geographic routing. The channel assignment strategy determines a cut-off point between the source and the destination, where the nodes on the two sides of the point (also referred as left segment and right segment) use different channels simultaneously. Note that we continue to assume that only one secondary communication can take place in one channel. However, the two different channels are assumed to be orthogonal, the communications on these two channels can occur at the same time. The outline of the channel assignment strategy is proposed below:

1) The source calculates the optimal cut-off point and the channel assignment for both sides of the cut-off point, based on the network parameters and the location of destination.
2) When the source formats the packet, it puts the location of the cut-off point, as well as the channel assignments on both sides of the cut-off point, in the packet header.
3) Upon receiving a packet, the intermediate node compares its location to the cut-off point. If it is on the left side of the cut-off point, it uses the channel assigned for the left segment, and vice versa.

We now discuss how the source can find the optimal cut-off point for a given communicating pair. Since we can use the two channels simultaneously, the segment that has larger hop count becomes the performance bottleneck. As a result, the end-to-end throughput is determined by the segment that has larger hop count. Let h^l and h^r be, respectively, the average hop count of the left and right segments. The end-to-end throughput is $r/\max\{h^l, h^r\}$ [6]. If we want to maximize the end-to-end throughput, we

[6]Here we assume that node density is high enough so that the path availability is 1. Therefore, the end-to-end throughput is only a function of hop count.

need to choose the channel combination that minimizes the the larger hop count of two segments, i.e. $\min(\max\{h^l, h^r\})$.

We use w to denote the location of the cut-off point, i.e. the cut-off point is at a distance of w from the secondary source. Let $h_1^l(w)$, $h_2^l(w)$ be the average hop count of left segment when using channel one and channel two respectively. Similar, let $h_1^r(w)$, $h_2^r(w)$ be the average hop count of right segment when using channel one and channel two respectively.

The value of $h_1^l(w)$ can be estimated by the mean hop count approximation procedure discussed in Section. III-C. Note that the use of the approximation procedure reduces the computation burden at the source. We have,

$$h_1^l(w) = \frac{w}{\frac{\sum_{(x,y)\in\Omega^l} Q_1(x,y)}{\sum_{(x,y)\in\Omega^l} 1}} \tag{35}$$

where $Q_1(x,y)$ is the hop distance of a node at location (x,y) when using channel one, and Ω^l is the set of discrete location points between the source and the cut-off point.

Similar for $h_2^r(w)$, we have

$$h_2^r(w) = \frac{D-w}{\frac{\sum_{(x,y)\in\Omega^r} Q_2(x,y)}{\sum_{(x,y)\in\Omega^r} 1}} \tag{36}$$

Let $T_{1,2}(w)$ be the end-to-end throughput of secondary pair if we split the routing path at w with the left segment uses channel 1 and the right segment uses channel 2. We have,

$$T_{1,2}(w) = \frac{r}{\max\{h_1^l(w), h_2^r(w)\}} \tag{37}$$

The optimal end-to-end throughput is

$$T_{1,2} = \max_w T_{1,2}(w) \tag{38}$$

and the optimal cut-off point for this channel assignment is:

$$w_1 = \arg\max_w T_{1,2}(w) \tag{39}$$

Similarly, let $T_{2,1}(w)$ be the end-to-end throughput of secondary pair if we split the routing path at w with the left segment uses channel 2 and the right segment uses channel 1.

The optimal end-to-end throughput for this particular channel assignment is:

$$T_{2,1} = \max_w T_{2,1}(w) \tag{40}$$

and the optimal cut-off point is

$$w_2 = \arg\max_w T_{2,1}(w) \tag{41}$$

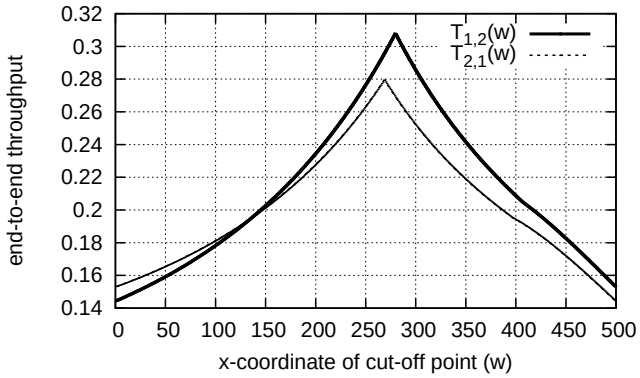

Fig. 15. End-to-end throughput as a function of cut-off point under ideal radio model.

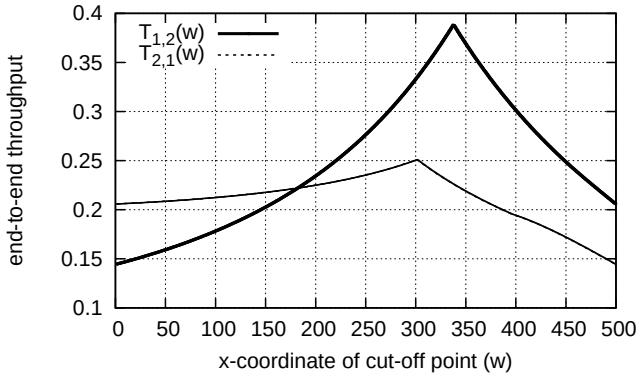

Fig. 16. End-to-end throughput as a function of cut-off point under fading radio model.

Therefore, if $T_{1,2} \geq T_{2,1}$, we should assign channel 1 to the left segment and channel 2 to the right segment, and use w_1 as the cut-off point. Otherwise, we assign channel 2 to the left segment and channel 1 to the right segment, and use w_2 as the cut-off point.

Note that, the above analysis is independent with radio models and can be applied to both ideal radio model and fading radio model. For an illustration, Fig. 15 shows the numerical results of the normalised throughput $T_{1,2}(w)$ and $T_{2,1}(w)$ as a function of w under ideal radio model. The normalisation is done with the link data rate r. The network parameters are the same as those used in preparing Fig. 14. Fig. 15 shows that, when using the channel 1 in the left segment, we can achieve the maximum throughput $T_{1,2} = 0.31r$ if the cut-off point is at 280. On the other hand, if we use the channel 2 in the left segment, we can achieve the maximum throughput $T_{2,1} = 0.28r$ when the cut-off point is at 270. Since $T_{1,2}$ is larger than $T_{2,1}$, we should assign channel 1 to the left segment and use 280 as the optimal cut-off point.

In this example, if we only use one channel for all intermediate nodes from the source to the destination, the best throughput that we can only achieve is $0.14r$. Therefore, by using this channel assignment, we can actually double the end-to-end throughput.

Fig. 16 shows the corresponding results under the fading radio model. It illustrates that the results have the similar pattern as the case in ideal radio model. However, in fading model, the optimal throughput is $0.39r$ and the cut-off is at 337, which are different with the values in ideal radio model. This is due to the fact that the hop distance of a node in two radio models is different, as shown in Fig. 7.

Note that, in this assignment, all intermediate nodes at the left side of cut-off point use the same channel, and the same for the right side segment. Consequently, only the secondary link that crosses over the cut-off point needs to perform channel switching operation (assume one radio interface is equipped at each secondary user). Therefore, our channel assignment can actually achieve the minimum channel switch overhead.

VI. Conclusion

Interference temperature (IT) model allows the secondary users to simultaneously utilize the channel with the primary users, which improves the channel access opportunities of cognitive radio networks. Since the secondary users in IT model use a reduced transmission power, a secondary source may need multi-hop communication with the destination. In this paper, we have quantitatively analyzed the end-to-end throughput of multi-hop whisper CRNs. We show that the secondary users can gain benefit from IT model in several scenarios, e.g. when the secondary pairs are located far from the primary pairs. We also illustrate that radio propagation model and node density have a significant impact on the performance of secondary users. The performance analysis of whisper CRNs can help us to design more efficient CRNs. In our technical report [20], we have discussed how one can apply the analysis results presented in this paper to design a multi-channel selection scheme, which can achieve higher performance and the minimum channel switching overhead. In this work, we have considered a localized routing protocol. In the future, we will investigate other advanced routing, MAC protocols or channel assignment schemes, and use the the performance results presented in this work as a comparison baseline.

References

[1] FCC, “Spectrum policy task force report,” ET Docket No. 02-135, November 2002.

[2] I. F. Akyildiz, W.-Y. Lee, and K. R. Chowdhury, “CRAHNs: Cognitive radio ad hoc networks,” *Ad Hoc Netw.*, vol. 7, no. 5, pp. 810–836, 2009.

[3] FCC, “Notice of inquiry and notice of proposed rulemaking,” ET Docket No. 03-237, November 2003.

[4] R. Zhang, "On peak versus average interference power constraints for spectrum sharing in cognitive radio networks," in *Proc. the 3rd IEEE Int. Sym. on New Frontiers in Dynamic Spectrum Access Net.*, Oct. 2008, pp. 1–5.

[5] T. C. Clancy, "Achievable capacity under the interference temperature model," in *Proc. the 26th Annual IEEE Conf. Comput. Commun.*, May 2007, pp. 794–802.

[6] ——, "Dynamic spectrum access using the interference temperature model," *Annals of Telecom.*, vol. 64, no. 7-8, pp. 573–592, August 2009.

[7] Q. Zhang, J. Jia, and J. Zhang, "Cooperative relay to improve diversity in cognitive radio networks," *IEEE Comm. Mag.*, vol. 47, no. 2, pp. 111–117, 2009.

[8] J. Zhang and Q. Zhang, "Stackelberg game for utility-based cooperative cognitiveradio networks," in *Proc. MobiHoc '09*, New Orleans, LA, USA, 2009, pp. 23–32.

[9] O. Simeone, Y. Bar-Ness, and U. Spagnolini, "Stable throughput of cognitive radios with and without relaying capability," *IEEE Trans. Commun.*, vol. 55, no. 12, pp. 2351–2360, 2007.

[10] O. Simeone, I. Stanojev, S. Savazzi, Y. Bar-Ness, U. Spagnolini, and R. Pickholtz, "Spectrum leasing to cooperating secondary ad hoc networks," *IEEE J. Select. Areas Commun.*, vol. 26, no. 1, pp. 203–213, 2008.

[11] Q. Chen, C. T. Chou, S. S. Kanhere, W. Zhang, and S. K. Jha, "Performance of multi-hop whisper cognitive radio networks," Accepted by IEEE DySPAN 2010, Jan. 2010.

[12] M. Xie, W. Zhang, and K.-K. Wong, "A geometric approach to improve spectrum efficiency for cognitive relay networks," *IEEE Trans. Wireless Commun.*, vol. 9, no. 1, pp. 268–281, Jan. 2010.

[13] M. Zuniga and B. Krishnamachari, "Analyzing the transitional region in low power wireless links," in *Proc. of First Annual IEEE Commun. Society Conf. Sensor and Ad Hoc Commun. and Net.*, Oct. 2004, pp. 517–526.

[14] G. Zhou, T. He, S. Krishnamurthy, and J. A. Stankovic, "Models and solutions for radio irregularity in wireless sensor networks," *ACM Trans. on Sensor Net.*, vol. 2, no. 2, pp. 221–262, 2006.

[15] B. Karp and H. T. Kung, "Greedy perimeter stateless routing forwireless networks (GPSR)," in *Proc. the 6th Annual Int. Conf. Mobile Comput. and Net.*, Boston, MA, USA, August 2000, pp. 243–254.

[16] H. Luo, F. Ye, J. Cheng, S. Lu, and L. Zhang, "A two-tier data dissemination in large-scale wireless sensor networks," *Wireless Net.*, vol. 11, pp. 161–175, Mar. 2005.

[17] S. Ratnasamy, B. Karp, L. Yin, F. Yu, D. Estrin, R. Govindan, and S. Shenker, "GHT: a geographic hash table for data-centric storage," in *Proc. the 1st ACM Int. Workshop Wireless Sensor Net. and Appl.*, Atlanta, GA, USA, September 2002, pp. 78–87.

[18] M. Haenggi, "On routing in random rayleigh fading networks," *IEEE Trans. Wireless Commun.*, vol. 4, no. 4, pp. 1553–1562, Jul. 2005.

[19] Q. Chen, S. S. Kanhere, and M. Hassan, "Hop count analysis for greedy geographic routing," CSE, UNSW, Sydney, Australia. UNSW-CSE-TR-0824, Available: ftp://ftp.cse.unsw.edu.au/pub/doc/papers/UNSW/0824.pdf, 2008.

[20] Q. Chen, C. T. Chou, S. S. Kanhere, W. Zhang, and S. K. Jha, "Multi-hop performance of whisper cognitive radio networks," UNSW-CSE-TR-1013, ftp://ftp.cse.unsw.edu.au/pub/doc/papers/UNSW/1013.pdf, 2010.